A 2.4

LINES OF FORCE OF A POINT CHARGE NEAR A SCHWARZSCHILD BLACK HOLE*†

Richard Squier Hanni

and

Remo Ruffini

Joseph Henry Laboratories
Princeton University
Princeton, New Jersey 08540

Abstract

The electric field generated by a charge particle momentarily at rest near a Schwarzschild black hole is analyzed using Maxwell's equations for curved space. By examining the multipole expansion fo the field about the center of the hole, we show that the transition to a Reißner-Nordstrøm hole is continuous. After generalizing the definition of the lines of force to our curved background, we compute them numerically and graph them with the charge at r = 4M, 3M, and 2.2M.

*Partially supported by National Science Foundation Grant #GP-30799X.

†Work partially based on the junior paper of R. S. Hanni submitted at Princeton University on December 11, 1970.

Introduction

The formalism for gravitational perturbations away from a Schwarzschild background has been developed by Regge and Wheeler[1]. It was extended by Zerilli[2], who has shown that perturbations corresponding to a change in the mass, the angular momentum, and the charge of a Schwarzschild black hole are well behaved. The decay of the non-well behaved perturbations has been investigated by Price[3]. He has shown that any multipole $\ell \geq s$, where s is the spin of the field being examined, gets radiated away in the late stage of gravitational collapse and will die as $t^{-(2\ell + 2)}$ for large t.

Instead of analyzing how higher order multipoles are radiated away, we focus on how the allowed transition from a Schwarzschild to a Reißner-Nordstrøm hole takes place through the capture of a charge particle in a given Schwarzschild background. In this paper we neglect the electromagnetic radiation emitted during the fall of the particle and consider a succession of configurations in which the particle is momentarily at rest at decreasing distances from the Schwarzschild horizon (r = 2m in geometrical units G = c = 1). The problem of examining the radiation emitted is, indeed, of great interest and has been presented elsewhere.

By considering the charge to be momentarily at rest, we were able to develop its electric field in a multipole expansion centered at the black hole. For any finite separation of the charge from the black hole, the far away observer will detect only the monopole term, the field corresponding to a Reißner-Nordstrøm solution. In the region near the charge, however, the contribution of higher multipoles is important and the lines of force are no longer radial.

As the charge approaches the horizon, the strength of all multipoles, except the monopole term, tends to zero. The lines of force assume more and more their Reißner-Nordstrøm pattern, only a very small region around the particle being significantly affected by the higher multipoles. The strengths of the multipole terms are derived as a function of the distance of the charge from the horizon. We generalize the concept of lines of force to curved space, and show that they are equivalent to the lines of constant flux. Finally, the concept of "induced charge" is introduced, and the smooth transition from the Schwarzschild to a Reißner-Nordstøm field is analyzed and a detailed graphical representation presented.

§1.2 Electrostatic Field in a Schwarzschild Background

The Schwarzschild metric can be expressed as:

$$(1)\quad ds^2 = -\left(1 - \frac{2M}{r}\right) dt^2 + r^2(d\theta^2 + \sin^2\theta\, d\phi^2) + \left(1 - \frac{2M}{r}\right)^{-1} dr^2 \quad .$$

In this background the only non-vanishing components of the electromagnetic field

$$(2.1)\quad F = F_{\mu\nu}\, dx^{\mu} dx^{\nu} \qquad \text{with} \qquad (2.2)\quad F_{\mu\nu} = A_{\nu,\mu} - A_{\mu,\nu}$$

of a particle momentarily at rest are:

$$(3.1)\quad F_{rt} = A_{t,r} = -F_{tr} \qquad \text{and} \qquad (3.2)\quad F_{\theta t} = A_{t,\theta} = -F_{t\theta} \quad .$$

Using the relation,

$$(4)\quad {}^*F_{\mu\nu} = \frac{\sqrt{-g}}{2}\, \varepsilon_{\mu\nu\delta\gamma} F^{\delta\gamma} \quad ,$$

where $\varepsilon_{\mu\nu\delta\gamma}$, we indicate the Levi Civita symbol and $g = \det|g_{\mu\nu}|$, we find that the only non-vanishing components of the dual electromagnetic tensor are

(5.1) $*F_{\theta\phi} = r^2 \sin\theta\, A_{t,r}$ and (5.2) $*F_{\phi r} = \sin\theta\, (1 - \frac{2M}{r})^{-1} A_{t,\theta}$.

The only non-vanishing component of the four current is

(6) $j^t = \frac{q}{2\pi r^2}\, \delta(r - a)\, \delta(\cos\theta - 1)$

where a is the value of the radial coordinate where the charge is located.

In covariant form Maxwell's equations are:

(7a) $F^{\alpha\beta}{}_{;\beta} = j^{\alpha}$ (7b) $*F^{\alpha\beta}{}_{;\beta} = 0$.

(Greek indices here and in the following go from 1 to 4). With (5) and (6) they yield a second order differential equation:

(8) $\frac{\partial(r^2 A_{t,r})}{\partial r}/r^2 + \frac{\partial(\sin\theta\, A_{t,\theta})}{\partial\theta}/r^2 \sin\theta\, (1 - \frac{2M}{r}) = j^t$

Using the exial symmetry of the problem and its regularity on the axis of symmetry, we can expand the solution in terms of Legendre polynomials

(9) $A_t = \sum_{\ell=0}^{\infty} f_\ell(r) P_\ell(\cos\theta)$.

The functions $f_\ell(r)$ satisfy, then, the second order differential equation

(10) $\frac{d}{dr}\left[r^2 \frac{d}{dr}(f_\ell(r))\right] - \ell(\ell+1) f_\ell(r)/(1 - \frac{2M}{r}) P^\ell(\cos\theta) = q\, \delta(r-a)\, \delta(\cos\theta - 1)/2\pi$

Substituting $u_\ell(r) = r f_\ell(r)$ and $z = r/2M$, Equation (10) takes the hyper-

geometric form:

(11) $\frac{d^2 u_\ell}{dz^2} - \frac{\ell(\ell+1)}{z(z-1)}\, u_\ell = 0.$

One of the two independent solutions of this equation is a polynomial of degree $\ell + 1$ with coefficients given by the recursion relation:

(12) $n\,(n+1)\,\alpha^\ell{}_{n+1} = [n(n-1) - \ell(\ell+1)]\,\alpha^\ell{}_n$.

The first few are:

(13.1) $u_0 = z$ (13.2) $u_1 = z(1 - z)$ (13.3) $u_2 = z(z-1)(2z-1)$.

To obtain the other independent solution v_ℓ we use the following relation, which follows form (11).

(14) $v_\ell\, u''_\ell - u_\ell v''_\ell = (v_\ell u'_\ell - u_\ell v'_\ell)' = 0$

or

(15) $v_\ell u'_\ell - u_\ell v'_\ell = c$

Integrating,

(16) $v_\ell = c\, u_\ell \int \frac{dz}{u_\ell^2}$.

From the explicit expressions for u_ℓ we obtain for v_ℓ :

(17.1) $v_0 = 1$ (17.2) $v_1 = z(1 - z)[2\ell n(z/(z-1)) - z^{-1} - (z-1)^{-1}]$

(17.3) $v_2 = z(z-1)(2z-1)^{-1} - (z-1)^{-1} + 6\ell n(z/(z-1)) - z^{-1}]$

and so on for larger ℓ. The most general solution for the potential can be cast in the form

$$(18)\quad A_t = \sum_{\ell} \frac{\alpha_\ell u_\ell(r) + \beta_\ell v_\ell(r)}{r} P_\ell(\cos\theta).$$

All of the u_ℓ's except the one corresponding to $\ell = 0$ vanish at the horizon. In the region inside the charge all the β_ℓ's must vanish, for the potential to be regular at the event horizon and vanish far away from the hole. Moreover, since $P_0(\cos\theta) = 1$, we can conclude that the horizon is an equipotential surface (A_t = const.).

For the potential to be regular as $r \to \infty$ all the α_ℓ's must vanish in the region outside the charge. As $r \to \infty$, the term v_0 is constant while all the other terms v_ℓ decreases as $r^{-\ell}$. The monopole term dominates at infinity. Gauss's law gives us the magnitude of the spherically symmetric electric field and thus the weighting coefficient for the monopole term, $\beta_0 = q$. The field far away approaches that of a point charge located at the center of the black hole.

§1.3 Matching Conditions and Strength of the Multipoles

In order to calculate the electric field we must evaluate the weighting coefficients: $\alpha_1, \beta_1, \alpha_2, \beta_2 \cdots$ Substituting the expansion (18) of A_t into Poisson's equation (10) we relate the discontinuity in the slope of each radial function to the amount of charge concentrated at $r = a$, $\theta = 0$, we have,

$$(19)\quad \frac{d^2u_\ell}{dz^2} - \frac{\ell(\ell+1)\,u_\ell}{z(z-1)} P_\ell(\cos\theta) = \frac{q}{2\pi z}\,\delta\left(z - \frac{a}{2M}\right)\,\delta(\cos\theta - 1)$$

Integrating over a thin shell containing the point $z = \frac{a}{2M}$ we obtain

$$(20)\quad \left[\frac{du_\ell}{dz}\right]_{z = \frac{a}{2M}} = -(2\ell + 1)q/(a/2M)$$

The continuity of the radial functions and the boundary conditions at the horizon and at infinity determine the weighting coefficients α_ℓ and β_ℓ uniquely. Because of the complexity of higher order terms we resort to numerical integrations to evaluate α_ℓ, β_ℓ, u_ℓ and v_ℓ.

Since the potential is continuous at the charge, we have

$$(21)\quad \alpha^\ell u_\ell(a) = \beta^\ell v_\ell(a) \int_0^a \frac{dz}{u_\ell^2(z)}\ .$$

The discontinuity in the field at the charge gives

$$\alpha^\ell u'_\ell(a) - \beta^\ell v'_\ell(a) = \frac{2\ell + 1}{q}$$

or for $\ell = 0$ $\beta^0 = q$ independent from the position of the charge and $\alpha^0 = q/a$

$$(22)\quad \text{for } \ell = 1 \quad \beta^1 = 3q(a - 1) \quad \alpha^1 = \frac{3qv_1(a)}{a}$$

$$(23)\quad \text{for } \ell = 2 \quad \beta^2 = 5q(2a - 1)(a - 1) \quad \alpha^2 = \frac{5qv_2(a)}{a}$$

Figure 1 shows the behavior of the radial functions for selected values of ℓ and selected values of the distance of the particle $a = 3M$, $a = 4M$ and $a = 6M$. While the monopole coefficient remains constant, all the other multipoles vanish as the particle approaches the horizon. The decay of the higher multipoles ($\ell > 0$) and the constancy of the monopole term determine the smooth transition from a Schwarzschild to a Reißner-Nordström geometry.

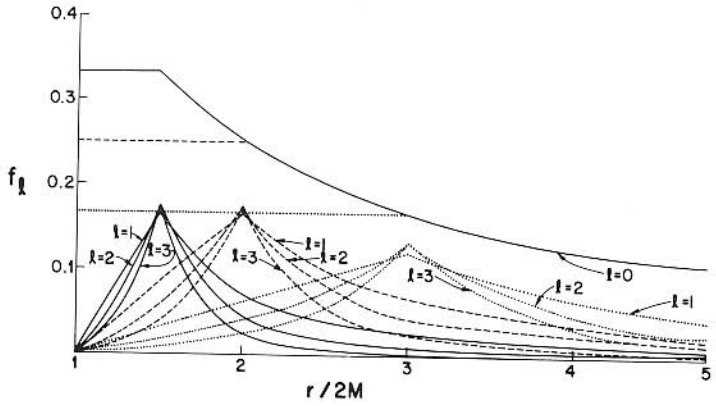

Fig. 1. Radial functions $f_\ell = (\alpha_\ell u_\ell(r) + \beta_\ell v_\ell(r))/r$ plotted as a function of the radial Schwarzschild coordinate r for selected values of ℓ and of the distance of the particle from the Schwarzschild surface ($\frac{a}{2M} = 2, 1.5, 1.1$). The strength of the multipoles $\beta_\ell = f_\ell r^{\ell+1}$ is constant for $= 0$ and increases with the distance of the particle from the black hole for $\ell > 0$.

§1.4 Definition of the Lines of Force

The generalization of Gauss's theorem to curved space is (4) given by the equation

(24) $\int_\vartheta {}^*F = 4\pi q$,

where q is the total charge withing the surface c_2 and

(25) ${}^*F = {}^*F_{\mu\nu}\, dx^\mu \wedge dx^\nu$.

Only the components (5.1) and (5.2) are non-zero, so

(26) ${}^*F = [r^2 \sin\theta \frac{\partial A_t}{\partial r}\, d\theta - (1 - \frac{2M}{r})^{-1} \frac{\partial A_t}{\partial \theta}\, dr] \wedge d\phi$.

If there exists a function Φ satisfying

(27) $\int_S {}^*F = \int_S d\Phi$,

then

(27.1) $\frac{\partial \Phi}{\partial \theta} = r^2 \sin\theta \frac{\partial A_t}{\partial r}$ and

(27.2) $\frac{\partial \Phi}{\partial r} = -(1 - \frac{2M}{r})^{-1} \frac{\partial A_t}{\partial \theta} \sin\theta$.

These conditions are met by the following expression for Φ :

(28) $\Phi = \sum_\ell - \frac{r^2}{\ell(\ell+1)} \frac{d}{dr} (\frac{f_\ell}{r}) \sin\theta \frac{dp_\ell}{d\theta}$.

We define a line of force as the locus of points with a given value of . At any given point, the slope of the line of force is:

(29) $\frac{dr}{d\theta} = -\frac{\partial \Phi}{\partial \Phi} / \frac{\partial \Phi}{\partial r} = (1 - \frac{2M}{r}) r^2 \frac{\partial A_t}{\partial r} / \frac{\partial A_t}{\partial \theta}$.

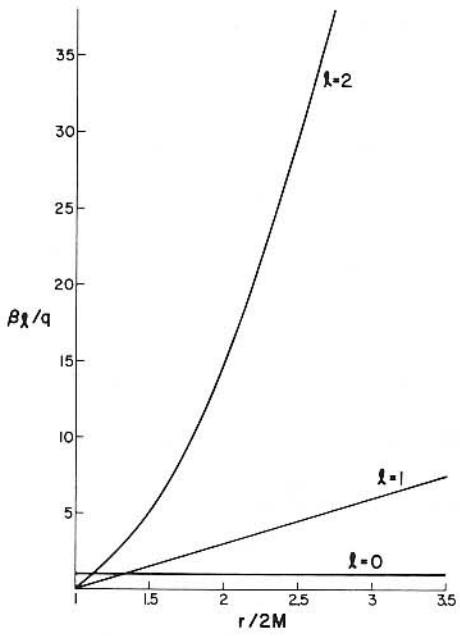

Fig. 2. Strength of the multipoles in units of the charge of the test particle q, as a function of the distance of the charge from the event horizon (r = 2M0. As $\frac{a}{2M} \to 1$, the monopole is constant, while the higher multipoles vanish.

This is equivalent to the operational definition of lines of force, introduced by Christodoulou and Ruffini[5]. They define a line of force as the line tangent to the direction of the electric force measured by an inertial observer momentarily at rest; this definition is also valid for stationary metrics. We then have

(30) $\epsilon_{ijk} F^{j}{}_{\alpha} \; u^{\alpha} \; dx^{k} = 0$ or

(30.1) $F^{r}{}_{t} u^{t} d\theta - F^{\theta}{}_{t} u^{t} dr = 0,$

which also gives expression (29) for the slope of the lines of force if we assume an inertial observer with four velocity $u^{\alpha} = (0,0,0,1)$.

Figures 3,4, and 5 show the lines of force in Schwarzschild coordinates, as the charged particle approaches the event horizon. When the charge is at r - 2.2m (Fig. 5), the field far away ($r \gtrsim 10M$) from the hole is nearly radial about the center of the hole. The monopole term clearly dominates. The contribution of the higher multipoles is dominant in the region near the charge.

The lines of force intersect the event horizon. We interpret this as a charge induced on the surface of the hole, which is proportional to the electric field normal to the surface. The total flux through the Schwarzschild surface, and thus the net induced charge is zero.

Let us assume that the point charge is positive. At angles less than a critical angle θ_{crit}, the induced charge is negative and the lines of force go toward the even horizon. At the critical angle there is no induced charge and the line of force is tangent to the Schwarzschild surface . At angles greater than the critical angle, the induced charge is positive and the lines of force are directed away from the horizon. Figure 6 shows the ratio

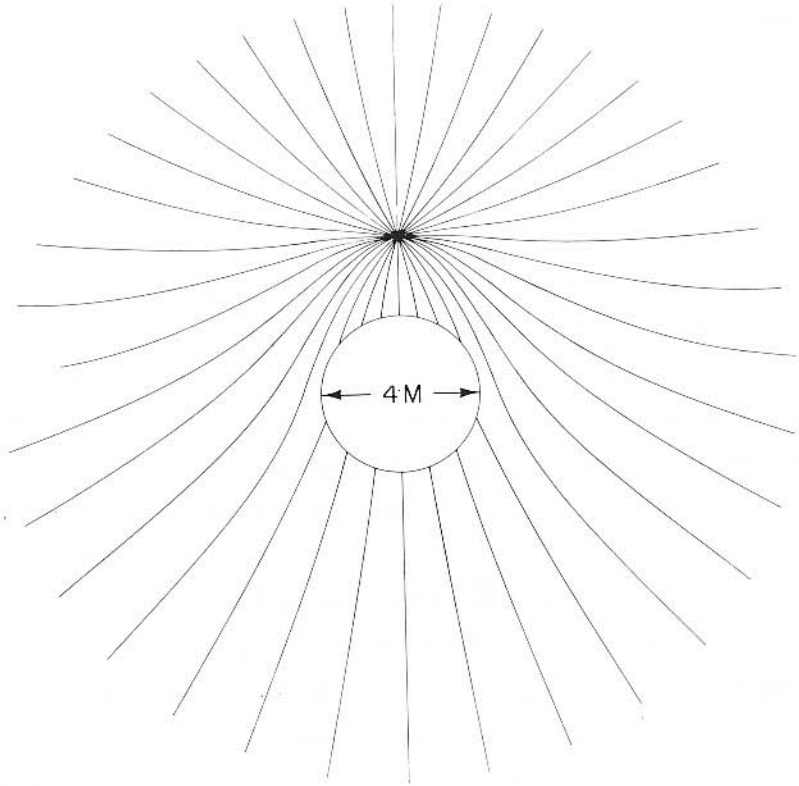

Fig. 3. Lines of force with the test charge momentarily at rest at r = 4M.

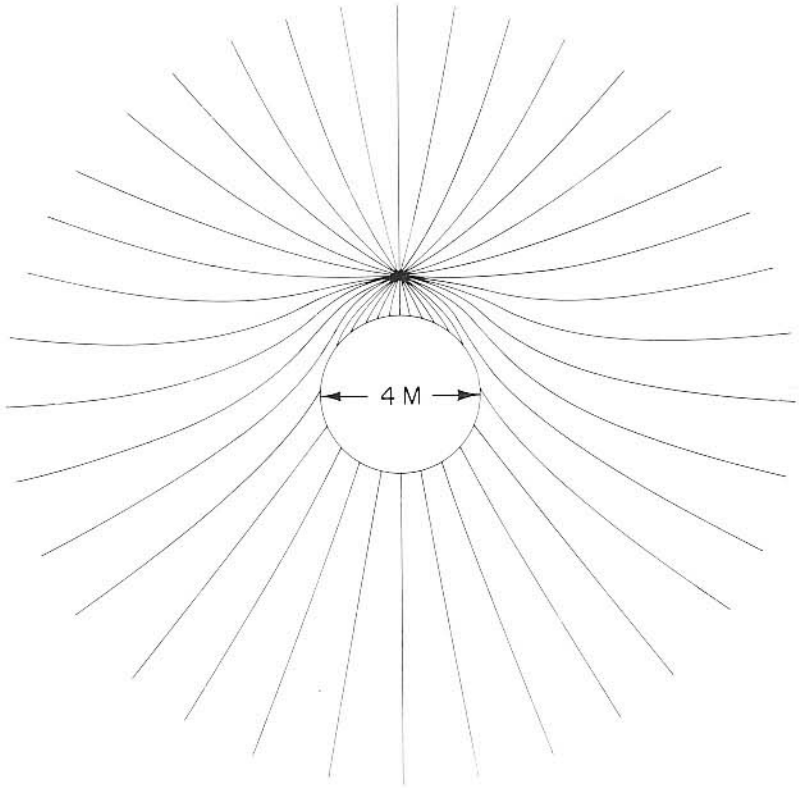

Fig. 4. Lines of force with the test charge momentarily at rest a r = 3M.

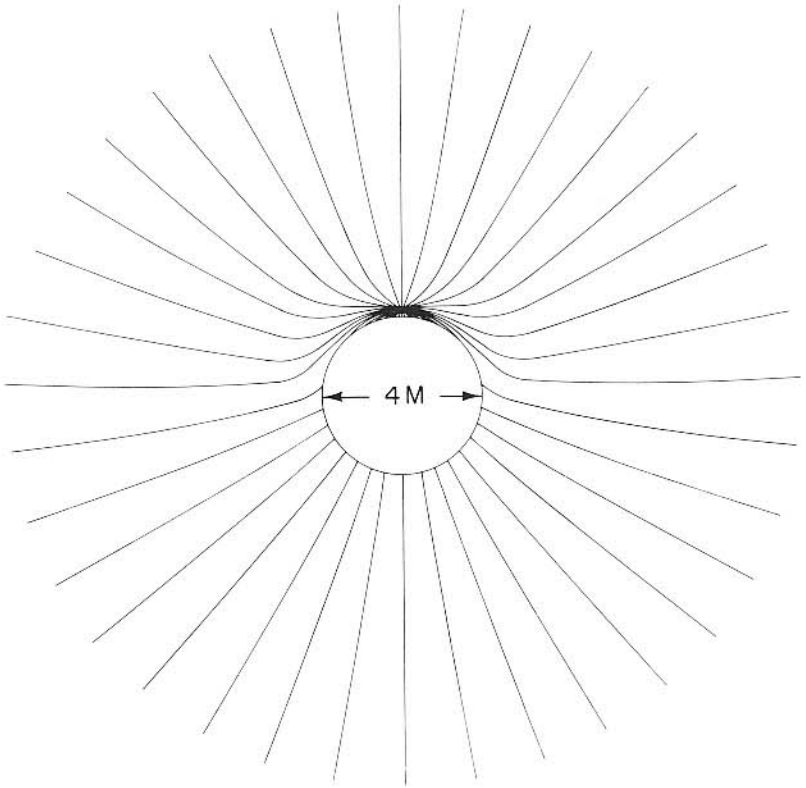

Fig. 5. Lines of force with the test charge momentarily at rest at r = 2.2M.

of the positive charge induced to that of the point charge and the critical angle, as functions of the radial coordinate of the charge.

The behavior of this induced charge shows clearly the smooth transition from a Schwarzschild to a Reißner-Nordstrøm hole. As the charge approaches the horizon, the magnitude of the induced charge approaches that of the point charge and the negative induced charge is crowded into a decreasingly small area around the pole. In contrast, the positive charge disperses itself more and more evenly over the rest of the surface of the sphere. The asymptotic limit of this evolution is a dipole with no strength at the pole, and a positive charge, equal in magnitude to that of the point charge, distributed evenly over the Schwarzschild surface. This charge distribution generates the monopole field of the Reißner-Nordstrøm solution.

It is essential to the interpretation of Figure 6, that the radial coordinate of a freely falling non-radiating particle with no angular momentum about the center of the hole decreases with time as:

$$r = 2m\ (1 + 4\ e^{-8/3}e^{-t/2m})$$

If the particle radiates away some of its energy, then the approach will be even slower. As seen by a far away observer, the charge approaches, but never reaches, the horizon (r = 2m). The ratio of the induced charge to the point charge approaches, but never reaches, one. The critical angle approaches, but never reaches zero. The coordinates velocity:

$$\frac{dr}{dt} = -\ 4e^{-8/3}e^{-t/2m}\ ,$$

decreases exponentially with time. Thus the system we have investigated is a good approximation of a charged particle in radial free fall, when the charge is sufficiently close to the hole.

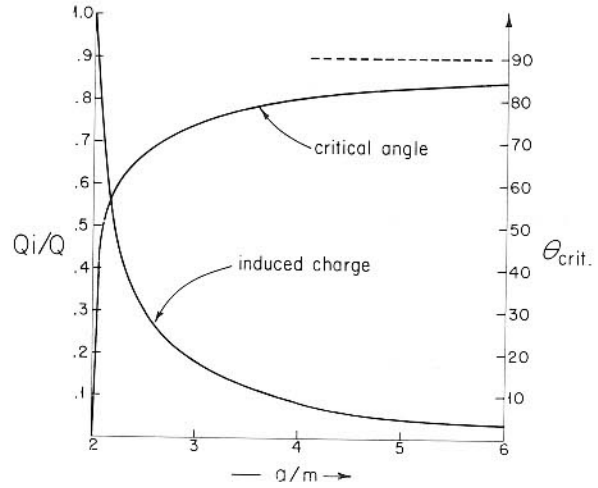

Fig. 6. The critical angle, θ_{crit}, where the line of force is tangent to the Schwarzschild surface and the induced surface charge vanishes, as a function of the radial coordinate of the test particle. Also given is the ratio of the charge induced on the black hole (see text) to the charge of the test particle.

Acknowledgment

It is a pleasure to acknowledge discussion on many aspects of this problem with John A. Wheëler.

References

1. T. Regge and J. A. Wheeler, Phys. Rev. 108, 1063, 1957.

2. F. Zerilli, Phys. Rev., D2, 2141, 1970.
F. Zerilli, Journ. Math. Phys. 11, 2203, 1970.
F. Zerilli, Phys. Rev. Lett. 24, 737, 1970.

3. R. H. Price, Phys. Rev. D10, 2419, 1972 and 10, 2439, 1972.

4. J. A. Wheeler, Geometrodynamics, Academic Press, 1962.

5. D. Christodoulou and R. Ruffini, "On the Electrodynamics of Collapsed Objects", unpublished.

A 2.5

Ultrarelativistic Electromagnetic Radiation in Static Geometries*

Remo Ruffini

Joseph Henry Physical Laboratories, Princeton, New Jersey 08540

and

Frank Zerilli†

University of North Carolina, Chapel Hill, North Carolina 27514

Radiation from ultrarelativistic circular orbits are, here, examined in the Reissner-Nordstrøm background, both by analytic and numerical techniques. Stable orbits with 100% binding and $v/v_{light} \sim 1$ exist. New insight and a physical explanation for the spectra recently considered by Davis, Ruffini, Tiomno and Zerilli are presented.

*Work partially supported by National Science Foundation Grant GP-30799X.

†Present address: Department of Astronomy, University of Washington, Seattle, Washington 98105

It has become more evident than ever that the proof for the existence of completely collapsed objects relies heavily on the observation of a continuous flux of radiation emitted by a stream of charged particles accreting toward the horizon[1]. Gravitational radiation, though extremely important, is expected to be emitted only in relatively rare and very short bursts of energy[2,3,4,5]. Quite apart from considering the problem of the energy emitted by a plasma in the ergosphere[6] of a magnetic black hole[7], which still presents superb difficulties both from a mathematical and a physical point of view,[8][9] we are here interested in the radiation emitted by a particle in circular orbit in the most general static geometry with regular horizon[10]. This analysis is also dictated by the need of a deeper understanding of the recent results of Davis, Ruffini, Tiomno, and Zerilli,[11] which clearly shows the existence of different behavior in the radiation field generated by particles of different spin in unbound ultrarelativistic circular orbits. Their results have been confirmed to indeed apply also in the limit of the highest multipoles and a very compact formula has been found to express the main features of the radiation fields [12]. We have, here, shown that the Reissner-Nordstrøm field greatly differs from the Schwarzschild or Kerr one, in the sense that orbit with 100% binding exist, they are stable, and reachable from particles of the characteristic size of an electron. For reasons we will explain we consider these orbits ultrarelativistic. We have also given, using the Ford-Hill-Wakano-Wheeler[13][14] approach the explicit form of the Green's functions for the ultrarelativistic unbound orbits in the Reissner-Nordstrøm geometry. Finally, we have used these two results to give a new insight in the nature of the spectral distribution discovered in Ref. (11).

(a) Orbit in Reissner-Nordstrøm geometry. The metric has the form

(1) $ds^2=g_{\mu\nu}dx^\mu dx^\nu=-(1-2M/r+Q^2/r^2)\,dt^2+r^2(d\theta^2+\sin^2\theta d\phi^2)+dr^2/(1-2M/r+Q^2/r^2)$

Greek indices goes from 0 to 3, G=c=1, M and Q are the mass and the charge characterizing the background geometry. For the energy and angular velocity of a test particle in circular orbit in the given geometry we obtain

(2.1) $\omega_o^2=(d\phi/dt)^2=M/R^3-Q^2/R^4-\varepsilon Q/R^3[\varepsilon Q/2R+(1-3M/R+2Q^2/R^2+\varepsilon^2Q^2/4R^2)^{1/2}]$

(2.2) $E/\mu=p_o=(1-2M/R+Q^2/R^2)/[\varepsilon Q/2R+(1-3M/R+2Q^2/R^2+\varepsilon^2Q^2/4R^2)^{1/2}]+\varepsilon Q/R$

Here $\varepsilon=q/\mu$ is the charge per unit mass of the test particle. The main results are shown in Fig. 1 for the geometry with Q/M=1. Not shown is an entire family of unstable circular orbits occuring for $\varepsilon > 1$ and at radii $r \leq [3M+(9M^2-8Q^2)^{1/2}]/2$. Details elsewhere. It is important to remark here that for every given value of $\varepsilon \leq 1$ there exists an orbit of maximum binding which corresponds to the last stable circular orbit; orbits with larger value of the radius are stable, while the ones with smaller radii. are unstable. The binding energy of a particle in the last stable orbits increases very rapidly with decreasing values of ε, its velocity tends toward the local value of the velocity of light. (See Fig. 1). In the entire family of unstable circular orbits, for fixed value of ε, the ratio between the velocity of the particle and the local value of the velocity of light increases monotonically for decreasing values of the radius and reaches the value of one at $r = r_p = 3M+(9M^2-8Q^2)^{1/2})/2$. Finally for large values of ε we can give asymptotic formulae for the radius and energy of the last stable circular orbit:

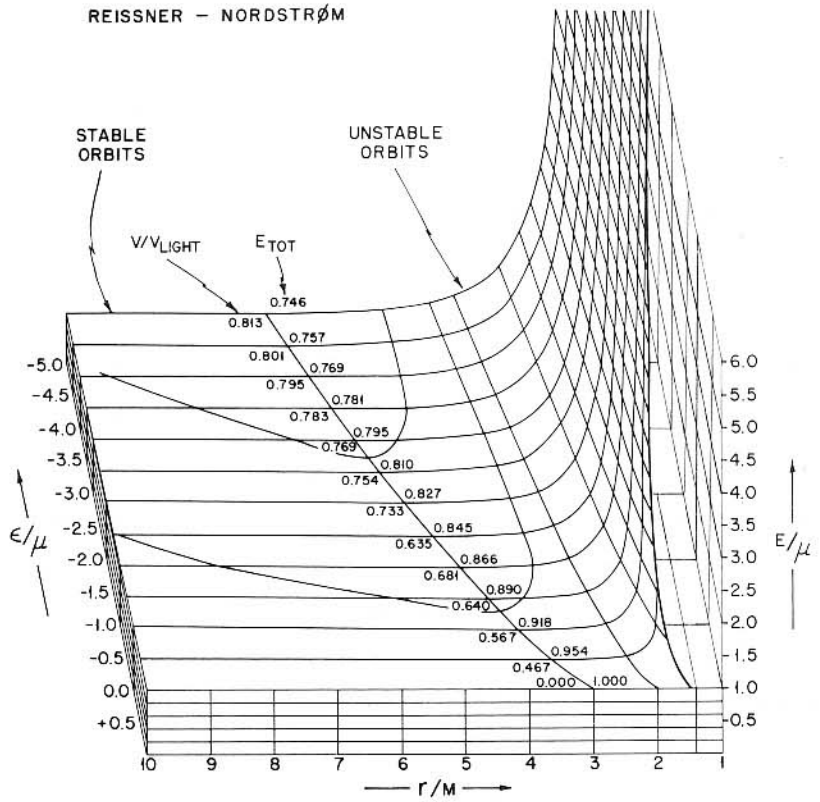

Fig. 1 Energy of circular orbits in an extreme Reissner-Nordstrøm field. E/μ is the energy, r/M the radial coordinate and $\varepsilon = q/\mu$ the charge of the particle; v/v_{light} is the velocity in the circular orbit measured with respects to the local value of the speed of light. The total energy is equal to the covariant p_o component of the momentum. The orbits with radii larger than the one corresponding to the last circular orbits are stable, the remaining ones are unstable.

(3.1) $R_{min} \sim \sqrt{2}\,(|\varepsilon Q|)^{2/3}$

(3.2) $E_{min}/\mu \sim \frac{3}{2}\,(2/|\varepsilon Q|)^{1/3}$.

These formulae apply in the limit $R_{min} >> M$ and $|\varepsilon Q| >> M$. Consider e.g. an electron ($\varepsilon = q/\mu = 2.04 \times 10^{21}$), a black hole of 1 solar mass and a net charge $Q/M \sim 10^{-3} \simeq 5 \times 10^{26}$ e.s.u., then $E_{min}/\mu \simeq 1.89 \times 10^{-7}$ and $R_{min} \simeq 0.39$ light years. For the evaluation of the net charge that should be expected on the surface of a collapsed object see Ref. (8).

(b) radiation from ultrarelativistic unbounded orbits.

Exploiting the symmetry properties of the equations and of the background geometry we can expand the covariant Maxwell equations in vector harmonics[15]. The two equations mastering the solution are for parity $(-1)^{\ell+1}$

$$(4.1)\quad b^{\ell m}{}_{,r^*,r^*} + \left(n^2\omega_o^2 - g_{oo}\,\frac{\ell(\ell+1)}{2}\right) b^{\ell m} = (-1)^m\,\frac{4\pi q\omega_o}{\ell(\ell+1)}\,\delta(m-n)P^{m\ell}(o)A_m^{\ell}\,\delta(r^*-r_o^*),_{r^*}$$

and for parity $(-1)^{\ell}$

$$(4.2)\quad a^{\ell m}{}_{,r^*,r^*} + \left(n^2\omega_o^2 - g_{oo}\,\frac{\ell(\ell+1)}{r^2}\right) a^{\ell m} = (-1)^m\,\frac{4\pi q\omega_o}{\ell(\ell+1)}\,\delta(m-n)P^{m+1}_{\ell}(o)\ .$$

where $[\ell(\ell+1)-m(m+1)]^{\frac{1}{2}} A_m^{\ell}\,\delta(r^*-r_o^*)$

$$A_m^{\ell} = [(2\ell+1)(\ell-m)!/(4\pi(\ell+m)!)]^{\frac{1}{2}}$$

The energy radiated is given by the formula

$$(5)\quad \frac{dE}{d\omega} = \sum_{\ell m}\frac{\omega^2}{2}\,\ell(\ell+1)\,\{|a_{\ell m}|^2 + |b_{\ell m}|^2\}$$

The solution of the problem is accomplished by finding the Green's functions of Eq. (4.1) and (4.2). We have solved this problem exactly by numerical techniques and we have given analytic expression for the Green's functions[14] for orbits near the top of the effective potential. To obtain the analytic

form of the approximate Green's function we can expand the effective potential for $r \sim r_b$ into a power series of r^*. Introducing then a new coordinate

(6) $\xi = \omega_\infty (\ell(\ell+1))^{1/4} r^* / \sqrt{k}$

with

$$k = r_p (3Mr_p - 4Q^2)^{-1/2} \text{ and } \omega_\infty^2 = (Mr_p - Q^2)/r_p^4$$

the homogeneous part of the equations (4.1) and (4.2) reduce to the well known equations generating the parabolic cylinder functions. The three cases $q > 0$, $q = 0$, $q < 0$ have to be treated separately. For the electric parity equations $(-1)^\ell$ we can introduce the following quantity:

(7)
$$\eta^{(e)} \begin{cases} k[1 + 4p + \tfrac{1}{2}|m|\varepsilon^2 Q^2/(Mr_p - Q^2)] & \text{for } qQ>0 \\ & \text{and } \delta \ll q^2Q^2/\mu^2M^2 \\ k[1 + 4p + M\delta r_p\,|m|/k^2\,(Mr_p - Q^2)] & \text{for } qQ = 0 \\ k[1 + 4p + M^2\delta^2\,|m|\,(\frac{1}{k^2} + \frac{9M^2-8Q^2}{\varepsilon^2Q^2})/(Mr_p - Q^2)] & \text{for } qQ < 0 \text{ and} \\ & \delta \ll q^2Q^2/\mu^2M^2 \end{cases}$$

with $\ell - m = 2p$.

for magnetic parity terms $(-1)^{\ell+1}$ we have

$$\eta^{(m)} = \eta^{(\ell)} + 2k \text{ and } \ell - m = 2p + 1$$

We are now able to write down the two linearly independent solutions of the homogeneous equations (4.1) and (4.2) for $r \sim r_p$:

$$(8)\quad R(\xi)=L(-\xi) = \frac{1}{\Gamma(\frac{1}{2} + i\frac{n}{2})} \int_0^\infty \exp[i\,\xi^2/2-(1-i)\,\xi t-t^2/2-(1/2-i\,\varepsilon/2)\ell nt]dt$$

where $R(\xi)$ is purely outgoing wave for $r^* \to +\infty$, and $L(\xi)$ a purely ingoing wave for $r^* \to -\infty$. Using Eqs. (6)(7) and (8) we can finally give the explicit form of the Green's functions and their derivatives

$$(9.1)\quad G(r^*,r_o^*) \simeq - \frac{i\,\Gamma(\frac{1}{4} + \frac{in}{4})\,k^{1/4}e^{-\pi\eta/8}e^{i\phi(r^*)}}{[4\sqrt{\pi}\,(\ell(\ell+1)^{3/8}\omega_\infty]}$$

and

$$(9.2)\quad \frac{\partial G(r^*,r_o^*)}{\partial r_o^*} = - \frac{1+i}{\sqrt{8\pi}} \quad \frac{\Gamma(\frac{3}{4} + i\,\frac{n}{4})e^{-\frac{\pi\eta}{8}}}{[\ell(\ell+1)]^{1/8}k^{1/4}}\, e^{i\phi}\,(r^*)$$

where the phase $\phi(r^*)$ is determined by matching $R(\xi)$ to a purely outgoing wave for large values of r^*. The final expression for the power radiated is

$$(10.1)\quad P_{\ell m}^{(e)} \simeq \frac{\omega_o^2\,q^2}{\sqrt{k}\,\pi^{3/2}} \quad \frac{(2p)!}{2^{2p}(p!)} e^{-\frac{\pi}{4}\eta^{(e)}}\,|\Gamma(\tfrac{3}{4} + \tfrac{i}{4}\,\eta^{(e)})|^2$$

for the magnetic terms of parity $(-1)^{\ell+1}$

$$(10.2)\quad P_{\ell m}^{(m)} \simeq \frac{\sqrt{k}}{2} \quad \frac{\omega_o^2}{2\omega_\infty} \quad \frac{\omega_o^2\,q^2}{\pi^{3/2}} \quad \frac{(2p+1)!}{2^{2p}(p!)^2}\; e^{-\frac{\pi}{4}\eta^{(m)}}\;|\Gamma(\tfrac{1}{4} + \tfrac{i}{4}\,(m)|^2$$

We can then immediately reach from the form of Eq. (10.1) and (10.2) the following general conclusions: the dominant term in the electric multipoles is the one with $\ell = m$ in the magnetic multipoles the one with $\ell - 1 = m$. In both cases the following term is down by a factor $e^{-2\pi k}$ with $k \sim 1$. The ratio of magnetic to electric power is

$$(11)\quad P_{\ell m}^{(m)}/P_{\ell m}^{(e)} = \frac{k}{2}\,(2p+1)\left\{\begin{matrix} 1-\varepsilon^2Q^2/(Mr_p-Q^2) \\ 1 \end{matrix}\right\} e^{-\pi k/2} \quad \left|\frac{\Gamma\,\frac{1}{4} + \frac{1}{4}\,in)}{\Gamma(\frac{3}{4} + \frac{1}{4}\,in)}\right|^2 \begin{matrix} \text{for } qQ > 0 \\ qQ \le 0 \end{matrix}$$

which is of the order of 10^{-2} or smaller. (See Fig. 2). For a test charge $q = \varepsilon\mu > 0$ we see that the $m = 1$ give the dominant contribution, each succeeding term being damped by a factor $\exp(-\pi k\varepsilon^2 Q^2 |m| / 2(Mr_p - Q^2))$. This behaviour in the spectrum is strictly connected with the fact that the radiation is emitted at values of $r < r_p$. Details will be given elsewhere.

Finally, let us here remark one of the main differences between this case and the one treated in Ref. (11). If $qQ < o$ the critical value of m at which the cutoff in the spectral distribution occurs is given by

$$(12)\quad m_{crit} = 4(Mr_p - Q^2)/[\pi k M^2 (1/k^2 + (9M^2 - 8Q^2)/\varepsilon^2 Q^2)]\delta^2$$

which radically differs from the one in Schwarzschild geometries. Details of the spectral distribution are given in (Fig. 2).

(c) Orbits with a constant value of v/v_{light}. To have a better understanding of the results presented in Ref. (11) we consider a sequence of configurations of equilibrium with a constant value of the ratio between the orbital velocity and the local value of the speed of light.

$$(13)\quad v/v_{light} = \omega_o/\omega_{light} = \omega_o R/(1 - 2M/R + Q^2/R^2)^{1/2}$$

here R is the radius of the circular orbit and ω_o is given by Eq. (2.1). These configurations correspond to different values of the test charge: the largest is the magnitude of the charge, the further away from $r = r_p$ they occur and the nearer to the family of last stable circular orbits. The main results of this analysis are summarized in Fig. 3, where two orbits with $v/v_{light} \sim 0.915$ and $\gamma = 2.48$ are considered. In one case the test charge has been chosen to have $q/\mu = -0.1$ and the orbit has a radius $r = 2.93$ M (very near the top of the potential barrier where our asymptotic

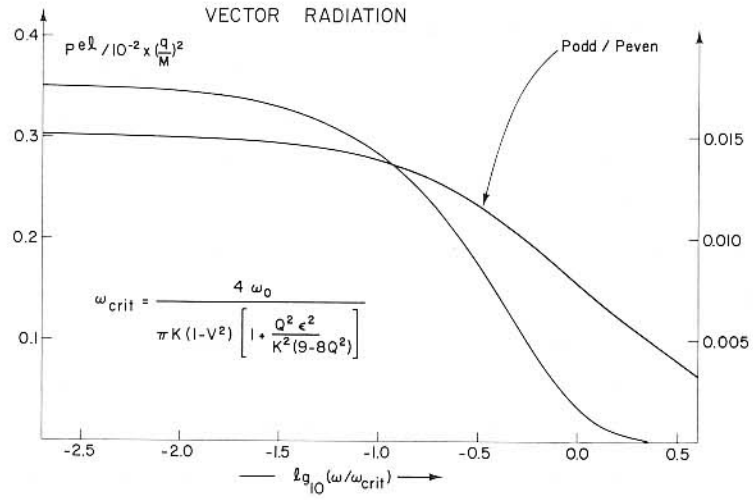

Fig. 2 Spectrum of electromagnetic energy radiated from a particle in ultrarelativistic orbits with radius $r \sim r_p$. The ratio between the odd$(-1)^{\ell+1}$ and even $(-1)^{\ell}$ parity contribution to the power radiated is also given as a function of the frequency.

treatment applies). In the other case, the test charge has been chosen to have $q/\mu = -10.0$ the radius of the orbit occurs now at $r = 6.795M$ where a full treatment of Eqs. (4.1) and (4.2) is needed, the expansion with the parabolic cylinder functions being inadequate in this range of values of r. We have in both cases used numerical techniques of integrations, details of which will be given elsewhere. The results are self-explanatory just by looking at Fig. 3!

It is worthwhile, however, to summarize at least the main conclusions:

(I) With the increase of the absolute value of the test charge the orbits move outward and the spectrum of the radiation emitted, rapidly recovers the main features of synchrotron radiation in flat space.

(II) When the particle is near the top of the potential barrier $r \sim r_p$, the highest multipoles (shorter wavelengths!!) are maximally affected and drastically damped[16]. The dipole term is only slightly damped.

(III) The radiation going inside the black hole, is of the order of fifty per cent, in the lowest multipoles limit in the first case considered ($q/\mu = -0.1$) and drops to one part in 10^3 in the case of $q/\mu = -10$.

These results, clearly, point out that the reason of the anomalous behaviour of the spectrum of the radiation for orbits near r_p, cannot be explained in terms of the relativistic velocity of the particle (special relativistic effect). It is, instead, mainly due to the fact that the radiation originates in a region very near the photon circular orbit ($r = r_p$). Photons beamed by the special relativistic effects are channelled in a "storage ring" at $r \sim r_p$ from which they leak out with varying time scales. The higher the multipole, the sharper and more effective the storage process is. This phenomenon, together with the large amounts of energy which goes inside the black hole, are, in our opinion, the

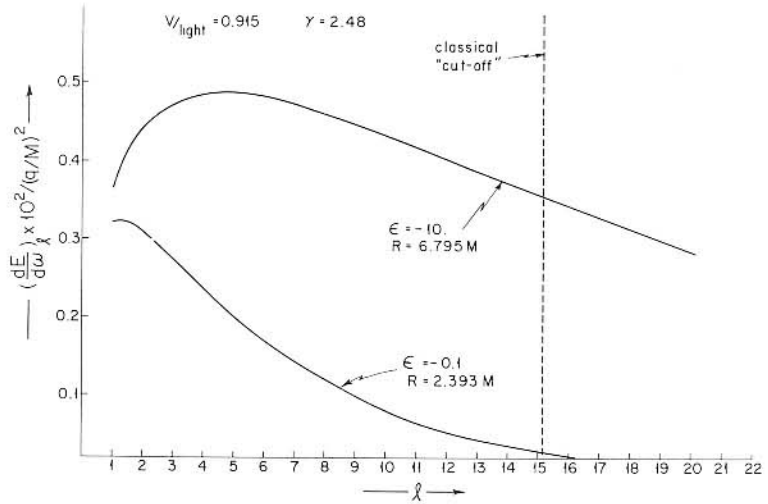

Fig. 3 Compared and contrasted are the spectral distributions of the radiation emitted by a charge in circular orbit near the top of the potential barrier $R \sim r_p (Q = -0.1)$ and one at $r = 6.795M$ $(Q = -10)$. Both orbits have the same value of the velocity measured with respect to the local value of the speed of light. The effects of the background geometry are in the case of $Q = -10$ is greatly reduced and the spectrum approaches the classical shape of synchrotron radiation.

physical reasons for the defocusing effects pointed out in Ref. 11. These effects clearly diminish when the radius of the orbit of the particle increases. Similar arguments apply to the spin 2 case, as well, the defocusing effect being there very much more pronounced, due to the fact, that the fundamental mode emission of the radiation is quadrupolar.

(1) R. Ruffini and J. A. Wheeler, Physics Today - January 1971, p. 39.

(2) M. Davis and R. Ruffini, Nuovo Cimento Lett. 2, 1165, 1971.

(3) M. Davis, R. Ruffini, W. Press, R. Price, Phys. Rev. Lett. 27, 1466, 1971.

(4) M. Davis, R. Ruffini, J. Tiomno - Phys. Rev. D12, 2932, 1972.

(5) R. Ruffini, Submitted to Phys. Rev.

(6) For the definition of ergosphere the e.g. R. Ruffini and J. A. Wheeler in "Cosmology from Space Platform" H. Moore and V. Hardy ESRO SP-52-Paris-1971.

(7) The ergosphere has been further generalized to the Kerr-Newman geometry by D. Christodoulou and R. Ruffini, Phys. Rev. 4,3552, 1971.

(8) R. Ruffini and A. Treves - Astrophysical Letters, in press.

(9) R. Leach and R. Ruffini - Ap. J. Lett., Submitted for publication

(10) W. Israel, Phys. Rev. 164 1776, 1967.

(11) M. Davis, R. Ruffini, J. Tiomno, F. Zerilli, Phys. Rev. Lett. 28, 1352, 1972.

(12) R. Breuer, R. Ruffini, J. Tiomno, C. V. Vishveshwara - Submitted to Phys. Rev.

(13) K. W. Ford, D. L. Hill, M. Wakano, J. A. Wheeler, Am. Phys. 7, 239 (1959).

(14) Analogous treatment for the Schwarzschild geometry has been given by C. W. Misner, R. A. Breuer, D. R. Brill, P. L. Chrzanowski, H. G. Hughes,III and C. M. Pereira, Phys. Rev. Lett. 28, 998, 1972.

(15) R. Ruffini, J. Tiomno, C. V. Vishveshwara, Nuovo Cimento Lett. 3, 211, 1972.

(16) This result manifestly contradict recent claim to have explained the "Nature of Gravitational Synchrotron Radiation" and the spectrum first founded in Ref. 11 by the inapplicability of the law of geometrical optics, in this regime. See e.g. D. M. Chitre and R. H. Price, Phys. Rev. Lett. 29, 185, 1972. If this was, indeed, the case the lowest multipoles should have been maximally affected and not viceversa!